• Basic Research •

Protective effects of upregulated *HO-1* gene against the apoptosis of human retinal pigment epithelial cells *in vitro*

Yu Hong[1], Yu−Ping Liang[1], Wei−Qi Chen[1], Liu−Xia You[2], Qing−Feng Ni[1], Xiu−Yun Gao[1], Xiao−Rong Lin[2]

[1]Department of Ophthalmology, the Second Affiliated Hospital of Fujian Medical University, Quanzhou 362000, Fujian Province, China

[2]Department of Clinical Laboratory, the Second Affiliated Hospital of Fujian Medical University, Quanzhou 362000, Fujian Province, China

Co-first authors: Yu Hong, Yu-Ping Liang, and Wei-Qi Chen

Correspondence to: Yu Hong. Department of Ophthalmology, the Second Affiliated Hospital of Fujian Medical University. No.34 Zhongshan North Road, Quanzhou 362000, Fujian Province, China. hongyuccd@163.com

Abstract

● **AIM:** To investigate the protective effect of heme oxygenase-1 (HO-1) against H_2O_2-induced apoptosis in human ARPE-19 cells.

● **METHODS:** The lentiviral vector expressing HO-1 was prepared and transfected into apoptotic ARPE-19 cells induced by H_2O_2. Functional experiments including cell counting kit-8 (CCK-8) assay, flow cytometry (FCM) and mitochondrial membrane potential assay were conducted.

● **RESULTS:** The ultrastructure of ARPE-19 cells was observed using transmission electron microscope (TEM). It was found that exogenous HO-1 significantly ameliorated H_2O_2-induced loss of cell viability, apoptosis and intracellular levels of reactive oxygen species (ROS) in ARPE-19 cells. The overexpression of HO-1 facilitated the transfer of nuclear factor erythroid-2-related factor 2 (Nrf2) from cytoplasm to nucleus, which in turn upregualted expressions HO-1 and B-cell lymphoma-2 (Bcl-2). Furthermore, HO-1 upregulation further inhibited H_2O_2-induced release of cysteinyl aspartate specific proteinase-3 (caspase-3).

● **CONCLUSION:** Exogenous HO-1 protect ARPE-19 cells against H_2O_2-induced oxidative stress by regulating the expressions of Nrf2, HO-1, Bcl-2, and caspase-3.

● **KEYWORDS:** retinitis pigmentosa; heme oxygenase-1; ARPE-19 cell; mechanism

DOI:10.18240/ijo.2021.05.03

INTRODUCTION

Retinitis pigmentosa (RP) as a clinical type in the most important hereditary blinding eye diseases shows significant clinical and genetic heterogeneity[1]. At present, more than one million in the world including over 400 000 Chinese suffer from it. Late RP patients show high risks of eye blindness and low vision, which must be given a high priority for its early diagnosis and treatment[2]. The degeneration of retinal photoreceptor cells and retinal pigment epithelial (RPE) cells is the main pathological change of RP[3]. RPE cells originating from the neuroectoderm present multiple biofunctions encompassing barrier effects, phagocytosis, anti-oxidative effects and involvements in visual cycle metabolism and secretion of growth factors, and trigger apoptotic responses to both photodamage and increased oxygen free radicals (OFR)[4]. RPE cell apoptosis is the most typical pathological feature of this malady. However, no effective treatment for RP has been found in clinic. Gene therapy of RP as one of the most promising treatments showing anti-apoptotic effects on RPE cells has been a hot spot[5], which is expected to improve the microenvironment for the benefit of the survival of RPE cells *via* upregulating neurotrophic factors or anti-apoptotic factors. As volumes of functional substances required for RPE cell regeneration are released, RPE cell apoptosis can be suppressed for restoring retinal function thereby. Besides, growth factors such as ciliary neurotrophic factor (CNTF) and brain-derived neurotrophic factor (BDNF) thwart RPE cell degeneration by blocking apoptosis[6]. Calcium antagonists enhance the expression of rhodopsin kinase, showing prevention effects against RPE cell degeneration[7]. And glutamate presents the same effect by inhibiting the process of apoptosis[8]. Therefore, among the effective factors above, screening out a gene of interest with fast and stable therapeutic effects against RPE apoptosis is the first imperative.

Heme oxygenase-1 (HO-1) is an evolutionarily conserved enzyme that breaks down heme into equimolar unstable iron,

carbon monoxide and biliverdin. The degradation of HO-1 into heme consumes 3 molecules of oxygen, indirectly triggering an inhibitory effect on oxidative damage[9], and bilirubin help eliminate OFR, oxygen, lipid hydroperoxide, *etc*. Such an endogenous antioxidant protects RPE cells against oxidative damage, prevents lipid peroxidation by binding to the cell membrane, and also reveals anti-complement and inhibitory effects on inflammatory mediators[10]. Promoting the outflow transport of intracellular iron is one of the mechanisms behind the cellular protection in the HO-1 system[11]. The strong adaptive response of HO-1 to various stimulating factors indicates its significance in the endogenous protective system with robust anti-apoptotic functions. Stocker[12] have found that HO-1 can be activated by various forms of stimuli to protect cells, showing the involvement in activating the nuclear factor erythroid-2-related factor 2 (Nrf2)/HO-1/B-cell lymphoma-2 (Bcl-2)/caspase-8 pathway against cell apoptosis. Zhang *et al*[13] have reported that salvianolic acid A can prevent apoptosis by triggering the Akt/mTORC1/Nrf2/HO-1 axis in an H_2O_2-induced ARPE-19 apoptosis model. Moreover, Zhu *et al*[14] have confirmed that hesperetin (HESP) can curb the H_2O_2-induced ARPE-19 apoptosis *via* stimulating the Keap1-Nrf2/HO-1 pathway, downregulate levels of reactive oxygen species (ROS) and reduced malondialdehyde (MDA), and upregulate levels of superoxide dismutase (SOD) and glutathione (GSH). In this study, we simulated the pathogenesis of RP, established a model of ARPE-19 apoptosis *in vitro*, and assessed the anti-apoptotic effects of HO-1 up-regulation against H_2O_2-induced ARPE-19 apoptosis.

MATERIALS AND METHODS

Reagents H_2O_2 (Sigma), DMEM medium (Sigma), fetal bovine serum (FBS; gibco), cell counting kit-8 kit (CCK-8; Sigma) and Annexin V-PV (BD company, USA) were used. The lentiviral system is composed of the plasmids as pSPAX2, pMD2G, and HMOX1 (Hanbio Biotechnology). The cells were divided into 4 groups: normal cultured ARPE-19 cells as the blank control group (BC group); H_2O_2 (209 µmol/24h)-induced apoptotic ARPE-19 cells as the pure injury group (PI group); lentiviral-mediated, empty vector transfected ARPE-19 cells as the Lv-EGFP-ARPE-19 group (Lv-EGFP group); and lentivirus-mediated *HO-1* gene transfected ARPE-19 cells as the Lv-HO-1-EGFP-ARPE-19 group (Lv-HO-1-EGFP group).

Cell Culture and Lentiviral-Vector Infection Human ARPE-19 cell line was purchased from ATCC (USA) and cultured in the DMEM medium containing 15% FBS at 37℃ and 5% CO_2. The full-length cDNA of *HO-1* gene was cloned and connected into the pHBLV-CMV-MCS-3flag-EF1-ZSgreen-puro plasmid. The recombinant lentivirus Lv-HO-1-EGFP vector was packaged and utilized to infect ARPE-19 cells. The cell line stably expressing HO-1 was obtained.

Cell Counting Kit-8 Assay The cells were fused with 80% to 90% of CCK-8 reagent with 10 µL in each well, and cultured for 4h. The optical density value was measured at an excitation wavelength of 420 nm using a microplate reader. And a fitting curve was depicted for the IC_{50} value of each group.

Flow Cytometry Analysis After the trypsin digestion of cultured ARPE-19 cells, the cells were collected and suspended with the buffer in an Annexin V-PV kit, with the cell concentration at $5×10^4$/L. Then the cells were collected according to the manufacturer's instructions, added with Annexin and PV, mixed and incubated for 20min, and cell apoptosis was detected by flow cytometry (FCM) within 1h. All steps above were carried out in a dark room. The test results were divided into 4 quadrants. The fourth quadrant represented the number of cells in the early stage of apoptosis, and the apoptotic rate was defined as follows: the apoptotic rate=the fourth quadrant apoptotic cells/total cell number×100%.

Mitochondrial Membrane Potential Assay Cells were seeded in 6-well plate when confluent to allow adherence. After 24h, the culture media were replaced with fresh media with drugs and blank control. After washed by PBS, the cells were collected by centrifugation at 2000 rpm for 5min and diluted at a dose of $1×10^6$/mL. The 1× incubation buffer was made up of 100 µL 10× incubation buffer and 900 µL sterilized ddH_2O and mixed to be prewarmed to 37℃. Meanwhile, JC-1 solution was made up of 1 µL JC-1 and 500 µL 1× incubation buffer and vortexed before use. Cells were diluted in 500 µL JC-1 solution and incubated at 37℃, 5% CO_2 for 15-20min. Then the cells were collected by centrifugation at 1000 rpm for 5min and washed twice with 1× incubation buffer. Finally, cells were resuspended in 500 µL of 1× incubation buffer and underwent FCM detection.

Transmission Electron Microscope Analysis Cell samples were selected and fixed for transmission electron microscope (TEM). After dehydration was performed three times, they were embedded in the pure acetone/embedding solution (volume ratio of 2:1) at room temperature for 3-4h, in the pure acetone/embedding solution (1:2) overnight at room temperature, and then in pure embedding solution at 37℃ for 2-3h. After that, the samples were cured overnight in the oven at 37℃, 45℃ for 12h, and 60℃ for 24h. The fixed samples were cut into thin sections (50-60 nm) using an LKB-1 ultra-thin slicer, followed by post-3% uranyl acetate-lead citrate double staining and TEM observation.

Immunoblotting Proteins of ARPE-19 cell samples were lysed in the SDS-containing electrophoresis buffer and protease inhibitors were added according to the protocol. The protein concentration was determined by the Bradford method (Bio-Rad Laboratories, Hercules, CA, USA). The samples were loaded into wells at the top of each gel and proteins were

A

```
NoName         1  merpqpdsmpqdlsealkeatkevhtqaenaefmrnfqkgqvtrdgfklvmaslyhiyvaleeeiernkespvfapvyfpeelhrkaale
5.19-h-hmox1  1107 merpqpdsmpqdlsealkeatkevhtqaenaefmrnfqkgqvtrdgfklvmaslyhiyvaleeeiernkespvfapvyfpeelhrkaale

NoName         271 qdlafwygprwqevipytpamqryvkrlhevgrtepellvahaytrylgdlsggqvlkkiaqkaldlpssgeglafftfpniasatkfkq
5.19-h-hmox1   837 qdlafwygprwqevipytpamqryvkrlhevgrtepellvahaytrylgdlsggqvlkkiaqkaldlpssgeglafftfpniasatkfkq

NoName         541 lyrsrmnslemtpavrqrvieeaktafllniqlfeelqellthdtkdqspsrapglrqrasnkvqdsapvetprgkpplntrsqapllrw
5.19-h-hmox1   567 lyrsrmnslemtpavrqrvieeaktafllniqlfeelqellthdtkdqspsrapglrqrasnkvqdsapvetprgkpplntrsqapllrw

NoName         811 vltlsflvatvavglyamletssrsgrgssvpsls dykddddkdykdddddkdykddddk-
5.19-h-hmox1   297 vltlsflvatvavglyamletssrsgrgssvpsls dykddddkdykdddddkdykddddk*
```

B
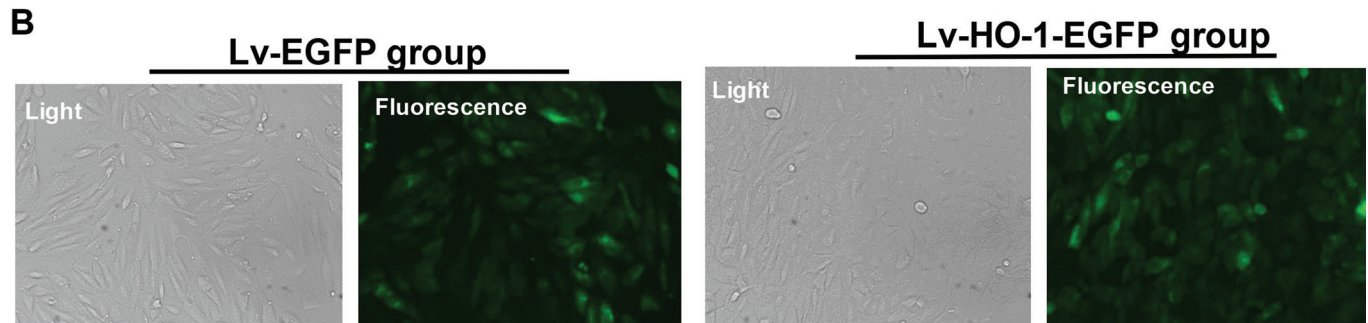
Figure 1 Validation of the constructed recombinant lentiviral plasmids by Sanger sequencing (A) and fluorescence microscope (B; 100×)
Sanger sequencing showed that the full-length *HO-1* cDNA was successfully cloned without gene mutations.

electrophoretically separated by SDS-polyacrylamide gel electrophoresis under reducing conditions. After target proteins electroblotted on PVDF membranes, they were incubated with primary antibodies including HO-1 (1:2000 dilution), Nrf2 (1:1000 dilution), Bcl-2 (1:2000 dilution) and cysteinyl aspartate specific proteinase-3 (caspase-3; 1:1000 dilution) and second antibodies. The bands were photographed using a gel imaging system (SYNGENE G: boxchemxr 5, UK).

Statistical Analysis Data were expressed as mean±standard deviation (SD), and analyzed using SPSS 20 software. When normality and homogeneity of variance were satisfied, the One-way ANOVA was used to compare the mean values between groups; if not, the Kruskal Wallis H test would be selected. A P value of <0.05 was considered statistically significant. Each experiment was repeated at least three times.

RESULTS

Validation of the Constructed Recombinant Lentiviral Plasmids The Sanger sequencing showed that the cloned fragment (the full-length *HO-1* cDNA) was identical to the target sequence (Figure 1A). ARPE-19 cells in the Lv-EGFP group and the Lv-HO-1-EGFP group showed significant EGFP expression at 24h following infection (Figure 1B), whereas no EGFP fluorescence was observed in the BC group and the PI group (data not shown). As *HO-1* shared the same region of the EGFP promoter, the observation of EGFP could indirectly hinted that the Lv-RNA-HO-1 vector successfully expressed HO-1-EGFP fusion protein.

HO-1 Up-regulation Increase the Survival of ARPE-19 Cells After subculture of ARPE-19 cells, the growth curves of Lv-HO-1-EGFP, Lv-GFP and BC groups were plotted according to culture days. The relative inhibition period appears at the first 3d; after that, cells in all groups proliferated exponentially and the difference between the groups was not statistically significant (Figure 2A; all P>0.05). The IC_{50} value of the survival rate in the Lv-HO-1-EGFP group was significantly higher than that in the Lv-EGFP group, and there was a nonsignificant difference in the IC_{50} value between the BC group and the Lv-EGFP group (Figure 2B). HO-1 over-expression significantly increased the survival rate of ARPE-19 cells, whereas mock infection revealed nonsignificant effects on the survival rate of ARPE-19 cells.

Exogenous HO-1 Reverse Apoptosis of ARPE-19 Cells As shown in Figure 3A and 3C, the total apoptosis rate by Annexin V-PV staining in the PI group was significantly higher than that in the BC group, indicating that the H_2O_2-induced apoptotic model was successfully established in ARPE-19 cells. There was a nonsignificant difference in the total apoptosis rate between the GF and PI group (Figure 3A and 3C). The apoptosis rate in the HO group was significantly lower than that in the Lv-EGFP group (Figure 3A and 3C). Correspondingly, the mitochondrial membrane potential assay by JO-1 also obtained similar results in line with the Annexin V-PV staining assay (Figure 3B and 3D).

HO-1 Rescued Cell Damage in ARPE-19 Cells The TEM assay revealed that the cells in the BC group were slightly damaged but the nuclei were intact (Figure 4A), whereas those in the PI group were severely damaged, and residual mitochondria and autophagosome-like structures were observed in the cytoplasm (Figure 4B). In the Lv-EGFP group, the cell damage was severe featuring disappeared organelles (Figure 4C). In the Lv-HO-1-EGFP group, the cell damage was obvious with a small amount of autophagic vacuoles
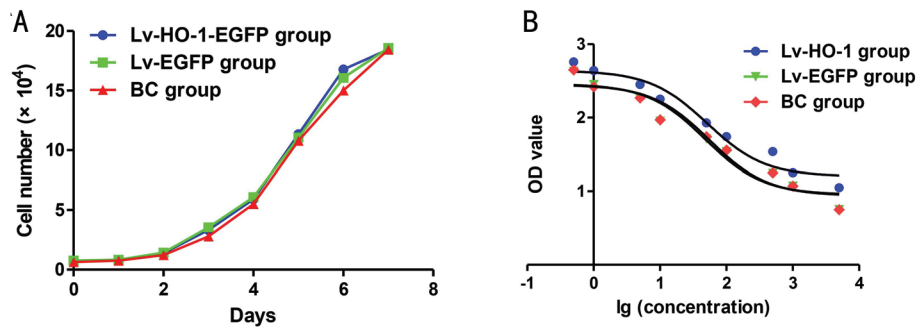
Figure 2 The survival analysis of ARPE-19 cells A: Cell growth curve by CCK-8 assay; B: The estimated IC$_{50}$ fitting curve based on the data from CCK-8 assay.
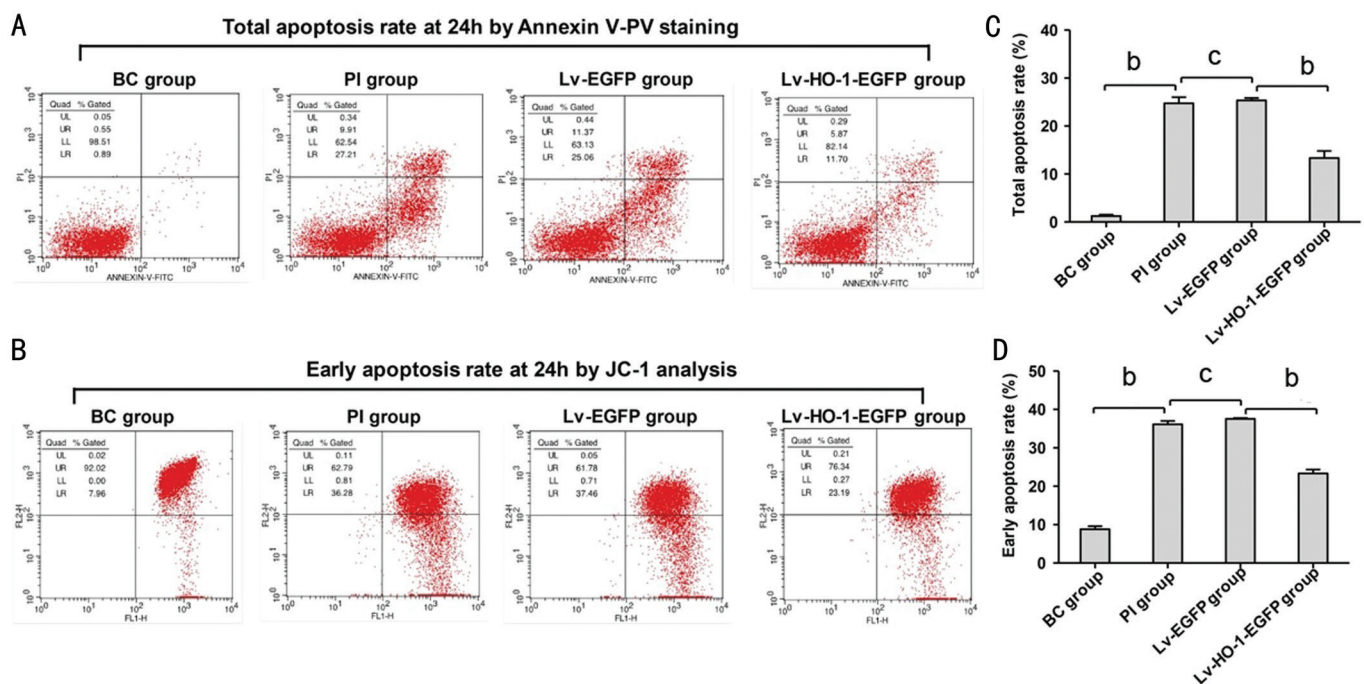
Figure 3 Injury of apoptosis rate at 24h by FCM A: Total apoptosis rate at 24h by Annexin V-PV staining; B: Early apoptosis rate at 24h by JC-1 analysis. BC group: Normal cultured ARPE-19 cells; PI group: H$_2$O$_2$ (209 µmol/24h)-induced apoptotic ARPE-19 cells. ^{c}P>0.05; ^{b}P<0.01.

(Figure 4D). No significant differences in the ultrastructure of ARPE-19 cells were found between the Lv-EGFP group and the PI group, indicating that the empty vector didn't affect the ultrastructure of ARPE-19 cells. However, the ultrastructure was more complete in the Lv-HO-1-EGFP group than that in the Lv-EGFP group, suggesting that HO-1 significantly curbed the apoptosis of ARPE-19 cells.

Exogenous HO-1 Triggered the Nrf2/HO-1/Bcl-2/caspase-3 Pathway Immunoblotting revealed that levels of HO-1, Nrf2 and Bcl-2 in the BC group were significantly higher than those in the PI group (P<0.01), and the caspase-3 protein level was significantly lower than that in the PI group (P<0.01; Figure 5). There were nonsignificant differences in expressions of HO-1, Nrf2, Bcl-2 and caspase-3 between the PI group and the Lv-EGFP group (P>0.05; Figure 5). However, levels of HO-1, Nrf2 and Bcl-2 in the Lv-HO-1-EGFP group were significantly higher than those in the Lv-EGFP group, with a lower level of

caspase-3 protein than that in the Lv-EGFP group (all P<0.01; Figure 5).

DISCUSSION

Retinal histopathology and immunocytochemistry have confirmed that RP originates from retinal photoreceptor cells, and the degeneration of ARPE-19 cells is the main pathological feature[3-4]. The cell degeneration and cell apoptosis in multiple clinical types of RP particularly attribute to apoptosis[15]. Scholars have investigated various treatments for RP, such as growth factors, ozone and retinal transplantation, however, all this has failed to effectively restore the normal function of the retina. Gene therapy directly targeting the pathogenesis of RP currently has been considered as a potential treatment[16-17].

In the current study, we choose H$_2$O$_2$ at the half-inhibitory concentration to simulate the *in-vivo* environment for apoptosis in an *in-vitro* model in ARPE-19 cells. We've found that the HO-1 protein acts as a protector of ARPE-19 cells against
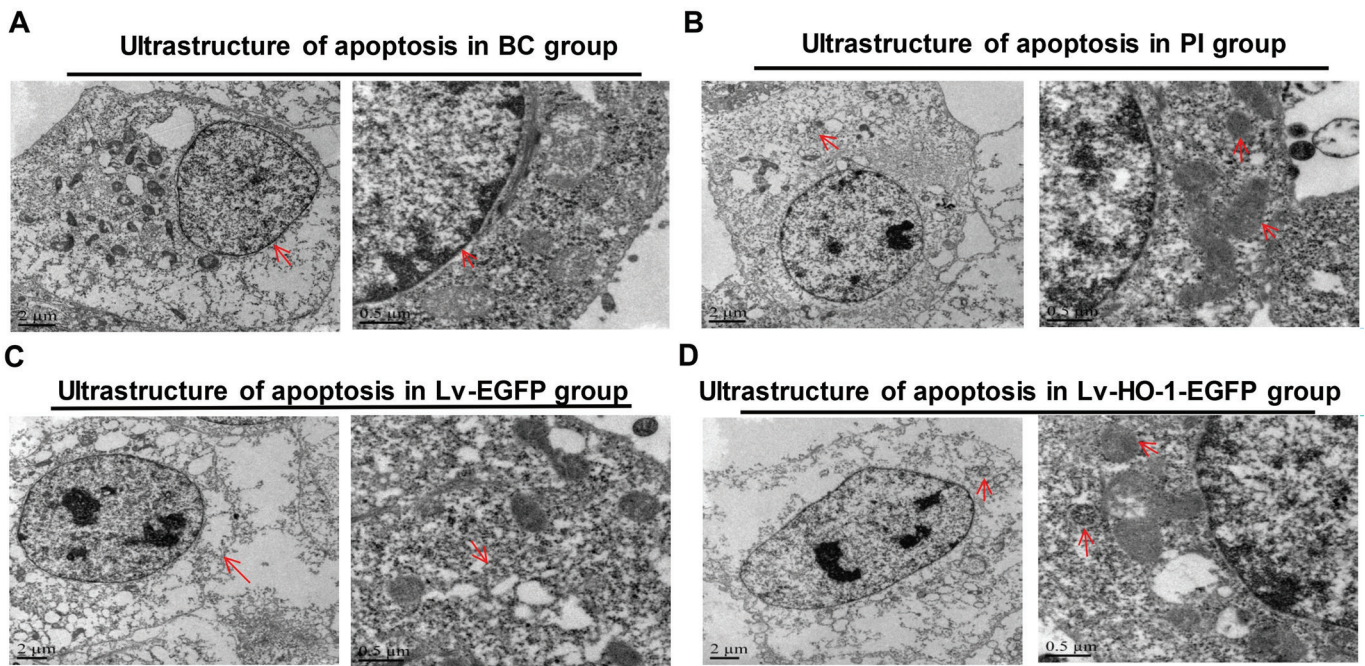
Figure 4 Differences in the ultrastructure of ARPE-19 cells by TEM A: In BC group, the red arrows show that cells were slightly damaged and the nuclei were intact; B: In PI group, the red arrows display that residual mitochondria and autophagosome-like structures were observed in the cytoplasm; C: In Lv-EGFP group, the red arrows indicate cell damage was severe with disappeared organelles; D: In Lv-HO-1-EGFP group, cell damage was obvious with a small amount of autophagic vacuoles.
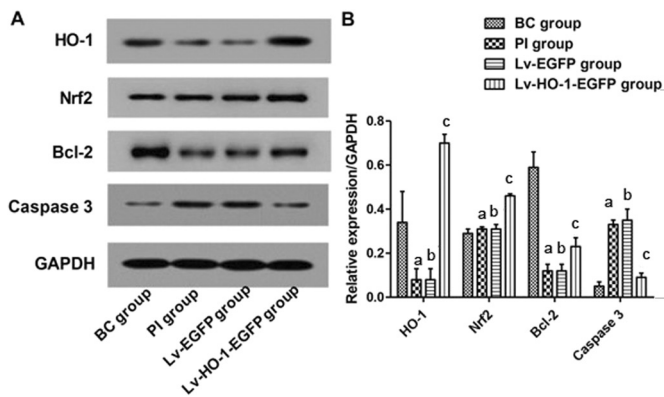
Figure 5 Expressions of HO-1, Nrf2, Bcl-2, and caspase-3 in each group A: Images for bands of the immunoblotting; B: Relative expressions of HO-1, Nrf2, Bcl-2, caspase-3 proteins to GAPDH. [a]Compared with blank control group, $P<0.01$; [b]Compared with simple injury group, $P>0.05$; [c]Compared with empty-body RPE group, $P<0.01$.

H_2O_2 toxicity and an enhancer for the apoptotic resistance of the cells.

To corroborate the protective effect of HO-1 overexpression against apoptosis, we have detected the apoptosis rate in ARPE-19 cells using FCM, and have found that HO-1 over-expression can significantly resist apoptosis. It is well known that the mitochondrial membrane potential is commonly used for coupling in the mitochondrial oxidative phosphorylation, and initially decreases prior to pathological changes in the mitochondrium. As this process is earlier than DNA fragmentation, mitochondrial membrane potential is usually used for detecting early apoptosis. Besides, to confirm the anti-apoptotic effect of HO-1 upregulation, FCM analysis has been adopted. It was found that the apoptosis rate in the Lv-HO-1-EGFP group was significantly lower than that in the Lv-EGFP group. This suggests that the *HO-1* gene transfection can significantly resist the early apoptosis in ARPE-19 cells.

Morphologically, TEM as the most reliable method is the gold standard for identifying apoptosis. We observe the ultrastructure of apoptotic cells in each group under TEM. The typical apoptotic changes occur in the ARPE-19 apoptosis model, featuring chromatin margins which are often distributed beneath the nuclear membrane. With the shape of the moon, the nucleus gradually falls out from the nuclear envelope into the cytoplasm or even becomes an apoptotic body outside the cell. The nuclei or apoptotic bodies of the apoptotic cells have a complete bilayer membrane wrap. At the same time, as the cytoplasm is highly concentrated with a shrinking cell body, the apoptotic cell is separated from neighbor cells, while the organelles in the plasma membrane and cytoplasm are still good. Sometimes the cytoplasm contains autophagic vacuoles. When the damage is serious, residual mitochondria alongside autophagy can be observed in the cytoplasm. In our study, the HO group presents superior anti-apoptotic effects over other groups. In conformity with the ultrastructure changes, it can be confirmed that *HO-1* gene overexpression significantly prevents ARPE-19 cells from apoptosis.

It has been reported that H_2O_2 can directly activate the inner mitochondrial membrane channel-the permeability transition pore (PTP), releasing cytochrome C from the mitochondria to the cytoplasm through an endogenous mitochondria-dependent pathway, leading to the activation of caspase-3[18-19]. In this study, we merely focus on the mitochondria-mediated, caspase-3 apoptotic pathway. Protein expressions of Nrf2, HO-1 and Bcl-2 in the HO group were significantly higher than those in the GF group, with significantly decreased caspase-3 protein levels in the HO group. This suggests that HO-1 upregulation inhibits ARPE-19 cell apoptosis through regulating the expressions of Nrf2, HO-1, Bcl-2, and caspase-3. By upregulation of HO-1, chrysin protects against LPS-induced cardiac dysfunction and inflammation by inhibiting oxidative stress[20]. The Nrf2-ARE pathway also can be activated by electroacupuncture, resulting in the upregulation of HO-1, which significantly reduces the severity of acute lung injury induced by endotoxin in rabbits[21]. Cyanoketene-induced Nrf2 activation reverses insulin resistance by inhibiting ER inflammation and oxidative stress, significantly reducing hepatic steatosis and the gene expressions required for lipid synthesis[22]. Pterostilbene can up-regulate Bcl-2 by activating Nrf2 and synchronously down-regulate Bax and caspase-3, so as to inhibit the apoptosis of pancreatic beta cells[23-24]. It is also reported that rosmarinic acid up-regulates Bcl-2 expression and protects ischemic stroke by up-regulating expressions of Nrf2 and HO-1 *via* the PI3K/Akt signaling pathway[25]. Hemin-1 facilitates HO-1 expression, bringing about the apoptosis of hepatic stellate cells by significantly suppressing Bcl-2, inhibiting the occurrence of liver fibrosis thereby[26]. In colorectal cancer cells, lncRNA-CASC2 regulates the pro-apoptotic effects of berberine by inhibiting the expression of Bcl-2 at the post-transcriptional level[27]. All these studies support the findings in our study.

In summary, our study demonstrates that H_2O_2 can induce mitochondrial membrane permeability transition and mitochondrial kinetics in ARPE-19 cells, resulting in mitochondrial pathway-related apoptosis triggered by Bax, cytochrome C, and caspase-3. However, lentivirus-mediated HO-1 upregulation can reduce the apoptosis stimulated by H_2O_2, improving the apoptotic resistance of ARPE-19, maintaining mitochondrial stability and counteracting H_2O_2-induced cell injury *via* regulating the expressions of Nrf2, HO-1, Bcl-2, and caspase-3 in ARPE-19 cells.

ACKNOWLEDGEMENTS

REFERENCES

1 Tsang SH, Sharma T. Retinitis pigmentosa (non-syndromic). *Adv Exp Med Biol* 2018;1085:125-130.

2 He YX, Zhang Y, Su GF. Recent advances in treatment of retinitis pigmentosa. *Curr Stem Cell Res Ther* 2015;10(3):258-265.

3 Zhang J, Gao F, Du C, Wang J, Pi X, Guo W, Li J, Li H, Ma Y, Zhang W, Mu H, Hu Y, Cui X. A novel RP2 missense mutation Q158P identified in an X-linked retinitis pigmentosa family impaired RP2 protein stability. *Gene* 2019;707:86-92.

4 Yan BJ, Wu ZZ, Chong WH, Li GL. Construction of a plasmid for human brain-derived neurotrophic factor and its effect on retinal pigment epithelial cell viability. *Neural Regen Res* 2016;11(12):1981-1989.

5 Bramall AN, Wright AF, Jacobson SG, McInnes RR. The genomic, biochemical, and cellular responses of the retina in inherited photoreceptor degenerations and prospects for the treatment of these disorders. *Annu Rev Neurosci* 2010;33:441-472.

6 Gozzelino R, Jeney V, Soares MP. Mechanisms of cell protection by heme oxygenase-1. *Annu Rev Pharmacol Toxicol* 2010;50:323-354.

7 Basiglio CL, Arriaga SM, Pelusa F, Almará AM, Kapitulnik J, Mottino AD. Complement activation and disease: protective effects of hyperbilirubinaemia. *Clin Sci (Lond)* 2009;118(2):99-113.

8 Recalcati S, Locati M, Marini A, Santambrogio P, Zaninotto F, De Pizzol M, Zammataro L, Girelli D, Cairo G. Differential regulation of iron homeostasis during human macrophage polarized activation. *Eur J Immunol* 2010;40(3):824-835.

9 Lenzi L, Coassin M, Lambiase A, Bonini S, Amendola T, Aloe L. Effect of exogenous administration of nerve growth factor in the retina of rats with inherited retinitis pigmentosa. *Vision Res* 2005;45(12):1491-1500.

10 Takano Y, Ohguro H, Ohguro I, Yamazaki H, Mamiya K, Ishikawa F, Nakazawa M. Low expression of rhodopsin kinase in pineal gland in Royal College of Surgeons rat. *Curr Eye Res* 2003;27(2):95-102.

11 Kitahara T, Ono K, Tsuchida A, Kawai H, Shinohara M, Ishii Y, Koyanagi H, Noguchi T, Matsumoto T, Sekihara T, Watanabe Y, Kanai H, Ishida H, Nojima Y. Impact of brachial-ankle pulse wave velocity and ankle-brachial blood pressure index on mortality in hemodialysis patients. *Am J Kidney Dis* 2005;46(4):688-696.

12 Stocker R. Induction of haem oxygenase as a defence against oxidative stress. *Free Radic Res Commun* 1990;9(2):101-112.

13 Zhang H, Liu YY, Jiang Q, Li KR, Zhao YX, Cao C, Yao J. Salvianolic acid A protects RPE cells against oxidative stress through activation of Nrf2/HO-1 signaling. *Free Radic Biol Med* 2014;69:219-228.

14 Zhu C, Dong YC, Liu HL, Ren H, Cui ZH. Hesperetin protects against H_2O_2-triggered oxidative damage via upregulation of the Keap1-Nrf2/HO-1 signal pathway in ARPE-19 cells. *Biomedecine Pharmacother* 2017;88:124-133.

15 Wong P. Apoptosis, retinitis pigmentosa, and degeneration. *Biochem Cell Biol* 1994;72(11-12):489-498.

16 Rakoczy EP, Lai CM, Magno AL, Wikstrom ME, French MA, Pierce CM, Schwartz SD, Blumenkranz MS, Chalberg TW, Degli-Esposti MA, Constable IJ. Gene therapy with recombinant adeno-associated vectors for neovascular age-related macular degeneration: 1 year follow-up of a phase 1 randomised clinical trial. *Lancet* 2015;386(10011):2395-2403.

17 Scalabrino ML, Boye SL, Fransen KM, Noel JM, Dyka FM, Min SH, Ruan Q, De Leeuw CN, Simpson EM, Gregg RG, McCall MA, Peachey NS, Boye SE. Intravitreal delivery of a novel AAV vector targets ON bipolar cells and restores visual function in a mouse model of complete congenital stationary night blindness. *Hum Mol Genet* 2015;24(21):6229-6239.

18 Razavinasab M, Moazzami K, Shabani M. Maternal mobile phone exposure alters intrinsic electrophysiological properties of CA1 pyramidal neurons in rat offspring. *Toxicol Ind Heal* 2016;32(6):968-979.

19 Bas O, Odaci E, Kaplan S, Acer N, Ucok K, Colakoglu S. 900 MHz electromagnetic field exposure affects qualitative and quantitative features of hippocampal pyramidal cells in the adult female rat. *Brain Res* 2009;1265:178-185.

20 Li XY, Li S,Wang Q, *et al*. Chrysin ameliorates sepsis-induced cardiac dysfunction through upregulating Nfr2/Heme oxygenase 1 pathway. *J Cardiovasc Pharmacol* 2021;77:491-500.

21 Yu JB, Shi J, Gong LR, Dong SA, Xu Y, Zhang Y, Cao XS, Wu LL. Role of Nrf2/ARE pathway in protective effect of electroacupuncture against endotoxic shock-induced acute lung injury in rabbits. *PLoS One* 2014;9(8):e104924.

22 Sharma RS, Harrison DJ, Kisielewski D, Cassidy DM, McNeilly AD, Gallagher JR, Walsh SV, Honda T, McCrimmon RJ, Dinkova-Kostova AT, Ashford MLJ, Dillon JF, Hayes JD. Experimental nonalcoholic steatohepatitis and liver fibrosis are ameliorated by pharmacologic activation of Nrf2 (NF-E2 p45-related factor 2). *Cell Mol Gastroenterol Hepatol* 2017;5(3):367-398.

23 Bhakkiyalakshmi E, Shalini D, Sekar TV, Rajaguru P, Paulmurugan R, Ramkumar KM. Therapeutic potential of pterostilbene against pancreatic beta-cell apoptosis mediated through Nrf2. *Br J Pharmacol* 2014;171(7):1747-1757.

24 Pihán P, Carreras-Sureda A, Hetz C. BCL-2 family: integrating stress responses at the ER to control cell demise. *Cell Death Differ* 2017;24(9):1478-1487.

25 Cui HY, Zhang XJ, Yang Y, Zhang C, Zhu CH, Miao JY, Chen R. Rosmarinic acid elicits neuroprotection in ischemic stroke via Nrf2 and heme oxygenase 1 signaling. *Neural Regen Res* 2018; 13(12):2119-2128.

26 Yang H, Chen B, Zhao Z, Zhang L, Zhang Y, Chen J, Zhang X, Zhang X, Zhao L. Heme oxygenase-1 exerts pro-apoptotic effects on hepatic stellate cells *in vitro* through regulation of nuclear factor-κB. *Exp Ther Med* 2018;16(1):291-299.

27 Dai W, Mu L, Cui Y, Li Y, Chen P, Xie H, Wang X. Berberine Promotes apoptosis of colorectal cancer *via* regulation of the long non-coding RNA (lncRNA) cancer susceptibility candidate 2 (CASC2)/ AU-binding factor 1 (AUF1)/B-Cell CLL/lymphoma 2 (Bcl-2) axis. *Med Sci Monit* 2019;25:730-738.